Am J Transl Res 2012;4(2):240-246
www.ajtr.org /ISSN:1943-8141/AJTR1203006

Original Article

Validation of transcatheter left ventricular electromechanical mapping for assessment of cardiac function and targeted transendocardial injection in a porcine ischemia-reperfusion model

Sharven Taghavi*, Jason M Duran*, Remus M Berretta, Catherine A Makarewich, Foram Udeshi, Thomas E Sharp, Hajime Kubo, Steven R Houser, Jon C George

*Cardiovascular Research Center, Temple University School of Medicine, Philadelphia, PA, USA. *Both authors contributed equally*

Received March 31, 2012; accepted April 15, 2012; Epub April 18, 2012; Published April 30, 2012

Abstract: Ischemic heart disease, despite advances in treatment, remains the major cause of mortality worldwide. NOGA 3D left ventricular electromechanical mapping allows accurate determination of cardiac function and precise identification of sites of injury. In a porcine model of ischemia-reperfusion injury, we validate the use of the NOGA mapping system for assessment of cardiac function along with the Myostar injection catheter for directed delivery of therapeutics to localized target sites in the setting of acute myocardial injury.

Keywords: Directed delivery of therapeutics , heart disease, transcatheter left ventricular electromechanical mapping , NOGA 3D

Introduction

As ischemic heart disease continues to be a major cause of morbidity and mortality [1], novel strategies for therapeutics are warranted. The NOGA mapping system (Biosense Webster, Diamond Bar, CA) utilizes a percutaneous catheter that uses an electromagnetic field to construct a three-dimensional endomyocardial map of the left ventricle measuring endocardial voltage potentials and myocardial contractility to distinguish between infarcted, ischemic, and normal myocardium [2]. Animal models have validated the use of electromechanical mapping (EMM) in accurately identifying areas of ischemia and infarction [3-5]. Studies have shown that EMM correlates well with other standard quantitative testing methods such as myocardial single photon emission computer tomography (SPECT) [6-8] and position emission tomography (PET) [7]. Subsequently, clinical trials have utilized EMM in humans to identify regions of the heart that are ischemic or scarred [9, 10].

Moreover, the NOGA system has been used to effectively guide the delivery of therapeutics, including growth factors via surgical approach [11] or with percutaneous catheter-based techniques [9, 12] in combination with the Myostar injection catheter (Biosense Webster, Diamond Bar, CA) via transendocardial injection [13-18].

While the NOGA system has been corroborated in the measurement of left ventricular volumes in a non-ischemic heart [19], its validation for the measurement of cardiac function during acute myocardial infarction (MI) has yet to be reported. The goal of this study was to determine the accuracy of the NOGA mapping system to measure cardiac function after MI and to determine its capacity to deliver putative therapeutics via transendocardial injection using the Myostar catheter during acute MI.

Materials and methods

Animals and anesthesia

All animal procedures were approved by the Temple University School of Medicine Institu-

tional Animal Care and Use Committee. Twelve male Yorkshire swine aged 6 months weighing 35-40 kg were used for the study. Anesthesia was induced using 6.0 mg/kg tiletamine (combined with zolazepam in Telazol; Fort Dodge, IA) given intramuscularly and was maintained using propofol (Diprivan, AstraZeneca, Wilmington, DE) administered intervenously at 50 mcg/kg/hour. Animals underwent endotracheal intubation and were maintained on assist control ventilation (tidal volume: 10-12 mL/kg, respiratory rate: 12-16 breaths/min, positive end-expiratory pressure of 5 cm H_2O, and inspiratory-expiratory ratio of 1:2). Blood oxygenation was closely monitored using continuous pulse oximetry and arterial blood gas samples taken every 30 minutes. Ventilation parameters were adjusted accordingly to keep arterial pH between 7.35-7.45 and arterial CO_2 between 35-45 mm Hg. Sodium bicarbonate was administered in 35 mEq doses to correct for acidosis. The electrocardiogram (EKG) was monitored throughout the procedure to detect any arrhythmias or cardiac instability requiring medical intervention.

Coronary angiography

The right femoral artery was cannulated using an 8 French percutaneous sheath (Boston Scientific, Natick, MA). A loading dose of 75 U/kg heparin was given prior to the introduction of the NOGA catheter, and maintenance doses of 30 U/kg heparin were given every 30 minutes throughout the procedure to prevent thrombotic complications. The left coronary artery was engaged using a 6 French JR4 guide catheter (Boston Scientific, Natick, MA) under fluoroscopic guidance and coronary angiography performed using Omnipaque 300 contrast agent (Nycomed-Amersham, New York, NY).

Ischemia-reperfusion myocardial infarction model

Prior to infarction, pigs were pre-treated with a prophylactic dose of 1 mg/kg amiodarone. A 3.0 x 12 mm Maverick balloon catheter (Boston Scientific, Natick, MA) was advanced over a Choice Floppy guidewire (Boston Scientific, Natick, MA) into the left anterior descending coronary artery (LAD) and inflated just distal to the first diagonal branch of the LAD in order to occlude blood flow to the anteroapical wall of the left ventricle. ST-segment elevation on EKG was used to assess the onset of infarction. The balloon inflation was maintained for 90 minutes of ischemia, and subsequently deflated allowing reperfusion, followed by recovery for 30 minutes.

During the MI and ischemia-reperfusion phase, advanced cardiac life support protocols were used to treat potentially fatal arrhythmias. The onset of sustained ventricular tachycardia on EKG was treated with additional 1 mg/kg boluses of amiodarone or 50 mg bolus of intravenous lidocaine.

NOGA 3D left ventricular electromechanical mapping and injection

NOGA mapping was conducted at baseline and after ischemia-reperfusion using a 8 French NOGA mapping catheter advanced into the left ventricle via the right femoral sheath. Three-dimensional maps were constructed using voltage readings recorded at the tip of the catheter after making contact with the endocardial surface of the ventricle at 80-100 discrete points. End-diastolic (EDV) and end-systolic volumes (ESV) were calculated from these electromechanical maps using NOGA software. After the ischemia-reperfusion phase, the Myostar percutaneous injection catheter was then used with NOGA guidance to perform transendocardial injection of fluorescent microspheres into the infarct border zone. Location of the injected microspheres was confirmed by direct visualization with ultraviolet light after sacrifice.

Transthoracic echocardiography

Transthoracic echocardiography (Echo) was performed at baseline and after ischemia-reperfusion using an Agilent Sonos 5500 sonograph. Short- and long-axis images were obtained in the 2D mode, and M-mode images were obtained in the short axis. All measurements including end diastolic dimension (EDD), end systolic dimension (ESD), EDV, ESV, and ejection fraction (EF) were calculated using guidelines from the American Society of Echocardiography [20].

Gross morphometric analysis

Following post-MI NOGA mapping and echo, the animal was sacrificed under general anesthesia. Cardiectomy was performed and the heart

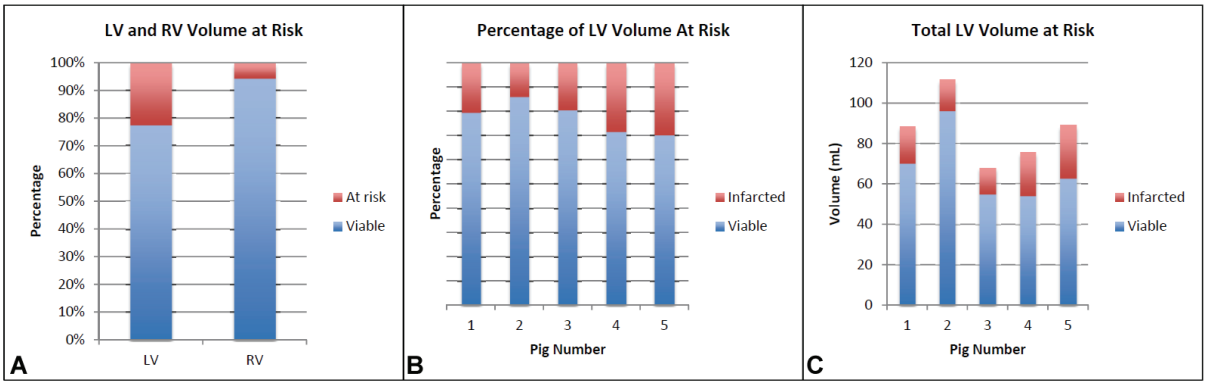

Figure 1. A) Comparison of LV and RV volume at risk after ischemia-reperfusion phase. B) Percentage and C) Total Volume at risk after ischemia-reperfusion.

rinsed in cold calcium-free Krebs-Henseleit Buffer (KHB) solution. The ventricles were carefully sectioned in the short-axis into 9-11 slices and the thickness of each slice measured at 3 independent points. The basal surface of each slice was photographed using a Nikon DS-F11 top-lit dissecting camera. The gross area at risk (AAR), identified by red and inflamed tissues, was measured using NIH Image J software, and volume at risk (VAR) was calculated by multiplying the AAR of each slice by the thickness of the slice. Net VAR of each heart was determined by the cumulative sum of VAR of each slice for a total value for each ventricle. Thicknesses of the anterior and posterior walls of the left and right ventricle and the thickness of the interventricular septum were also determined using gross morphometric measurements.

Statistical analysis

Paired student's t-test was used to examine differences between paired groups. Analysis of variance was used to examine differences between non-paired groups. A p-value less than 0.05 was considered significant. All data are expressed as mean ± standard error of mean (SEM).

Results

Procedure and mortality

There were 12 study animals with one death (8.3%) from refractory ventricular fibrillation during the ischemia phase of the procedure. NOGA mapping, echo, and gross morphometric analysis was available for 5 animals. Two animals were used as shams. Two animals, in the early phase of the study, were excluded due to insufficient data points for adequate EMM. One pig was excluded due to abnormal heart function at baseline while another was excluded due to inability to occlude the LAD for adequate ischemia.

Gross morphometric findings with ischemia-reperfusion model

VAR was calculated after ischemia-reperfusion (n=5) in both the left and right ventricle (**Figure 1**). Mean LV volume was calculated to be 86.7±7.4 ml. After the ischemia-reperfusion phase, VAR was determined to be 19.2±2.3 ml (22.6%±3.0%). Right ventricular volume was calculated at 38.9±7.0 ml with VAR being 2.0±0.2ml (5.6%±0.2%). Anterior and posterior wall thickness after ischemia-reperfusion was compared to non-infarcted sham animals (n=2). Anterior wall thickness significantly increased (1.38 vs. 1.14, p=0.029) and posterior wall had no significant difference (1.25 vs. 1.12, p=0.336).

Echo findings with ischemia-reperfusion model

Echo findings (n=5) showed significant increase in EDD (15.4%), ESD (37.6%), EDV (34.5%), and ESV (130.0%) as seen in **Table 1**. Anterior wall thickness (AWT) and posterior wall thickness (PWT) also increased at systole and diastole. Systolic AWT increased 14.6% while systolic PWT increased 18.0%. Significant decreases were seen in EF (39.2%) and fractional shortening (FS) (25.7%). Representative M-mode images can be seen in **Figure 2**.

Table 1. Transthoracic Echo Data (n=5)

	Baseline	Ischemia-Reperfusion	p-value
EDD (cm)	3.63±0.19	4.19±0.18	0.008
ESD (cm)	2.10±0.10	2.89±0.19	0.048
FS (%)	42.1%±1.4%	31.3%±3.2%	0.007
EDV (ml)	40.9±3.1	55.0±2.2	0.001
ESV (ml)	14.0±1.0	32.8±1.4	<0.001
SV (ml)	26.9±2.3	22.2±2.5	0.079
EF (%)	65.6%±1.6%	39.9%±3.5%	0.001
Systolic AWT	2.06±0.08	2.36±0.07	0.044
Diastolic AWT	2.10±0.10	2.89±0.23	0.083
Systolic PWT	1.41±0.08	1.72±0.08	0.045
Diastolic PWT	1.64±0.11	1.87±0.11	0.004

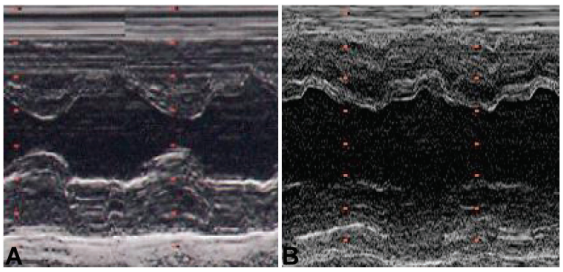

Figure 2. M-mode short axis images at baseline (left) and after ischemia-reperfusion (right).

Comparison of echo to gross morphometric findings

Wall thickness measured by echo were compared to those by gross morphometric analysis, and found to be greater as measured by echo in both systole and diastole. Wall thickness measured by echo at baseline (n=5) was significantly greater than sham animals measured by gross morphometric analysis (n=2) before ischemia reperfusion for both diastolic AWT (1.41 vs. 1.14 cm, p=0.247) and PWT (1.64 vs. 1.12 cm, p=0.080). When using baseline echo values in systole, AWT (2.06 vs. 1.14 cm, p<0.001) and PWT (2.10 vs. 1.12 cm, p=0.004) were still greater than gross morphometric measurements. Post ischemia-reperfusion echo measurements (n=5) were also compared to post ischemia-reperfusion gross morphometric measurements. Echo diastolic AWT (1.72 vs. 1.38 cm, p=0.033) and PWT (1.87 vs. 1.25 cm, p<0.001) were greater than those measured by gross morphometric analysis. Similarly, echo systolic measurements were also greater for AWT (2.36 vs 1.38 cm, p<0.001) and PWT (2.38 vs. 1.25 cm, p<0.001).

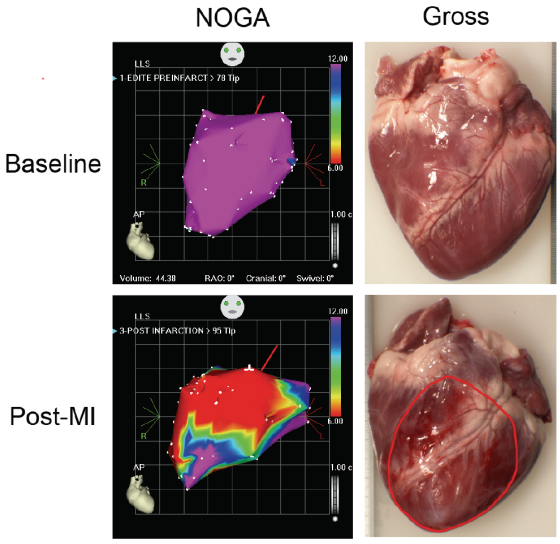

Figure 3: NOGA map (left) of a normal left ventricle showing normal myocardium in purple. This map correlates with the gross image (right) of the same normal heart. NOGA map (left) of the left ventricle 1 hour post ischemia-reperfusion showing infarcted myocardium in red. This map correlates with the gross image (right) of the same infarcted heart, with the infarct circled in red.

Comparison of NOGA to gross morphometric findings

NOGA generated infarct maps were consistent with direct in-vitro measurements of infarct size (**Figure 3**), demonstrating accuracy in mapping the ischemic portion of the heart. Localized injection of fluorescent microspheres into the ischemic border zone using NOGA and the MyoStar catheter were confirmed to be at the MI border zone by direct visualization in explanted tissue (**Figure 4**).

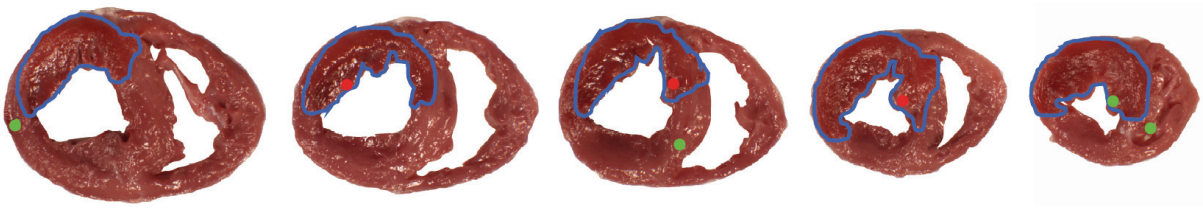

Figure 4. Fluorescent microspheres were injected within the infarct core (red) or at the infarct border zone (green) using the NOGA-guided Myostar injection catheter. After dissecting the heart, microspheres of each color were identified grossly under ultraviolet light. Microsphere injection sites were identified in the middle five sections of the infarct zone. Outlined in blue is the myocardium at risk.

Comparison of Echo measurements to NOGA

Comparison of echo and NOGA measurements (n=5) showed no significant differences (**Figure 5**). Baseline EF (65.6%±1.6% vs. 67.1%±1.5%, p=0.178) and post-MI EF (39.9%±3.5% vs. 35.4%±2.1%, p=0.267) were not different as measured by echo or NOGA. Comparison of EDV at baseline (40.9±3.1 vs. 50.0±8.1, p=0.391) and after ischemia-reperfusion (55.0±2.2 vs. 55.7±4.9, p=0.895) was also not different. ESV as measured by both modalities at baseline (14.0±1.0 vs. 16.8±3.4, p=0.448) and post-MI (32.8±1.4 vs. 36.2±3.9, p=0.307) was not significantly different. Stroke volumes were also similar before (26.9±2.3 vs. 33.1±4.9) and after ischemia-reperfusion (22.2±2.5 vs. 19.6±1.5, p=0.474).

Discussion

Coronary ischemia by balloon occlusion followed by reperfusion in this swine model closely simulates acute MI followed by revascularization in clinical setting. It is an ideal model for testing novel strategies for measuring cardiac function and delivering therapeutics in ischemic heart disease. The NOGA mapping device, in conjunction with the Myostar catheter, provides both diagnostic and therapeutic properties.

The NOGA map accurately identifies ischemic or scarred myocardium [6-8] and has been used in clinical applications [9, 10]. Our findings additionally confirm that it is an effective and accurate method for measuring cardiac function and heart volumes both at baseline and after ischemic injury. The NOGA catheter detected a

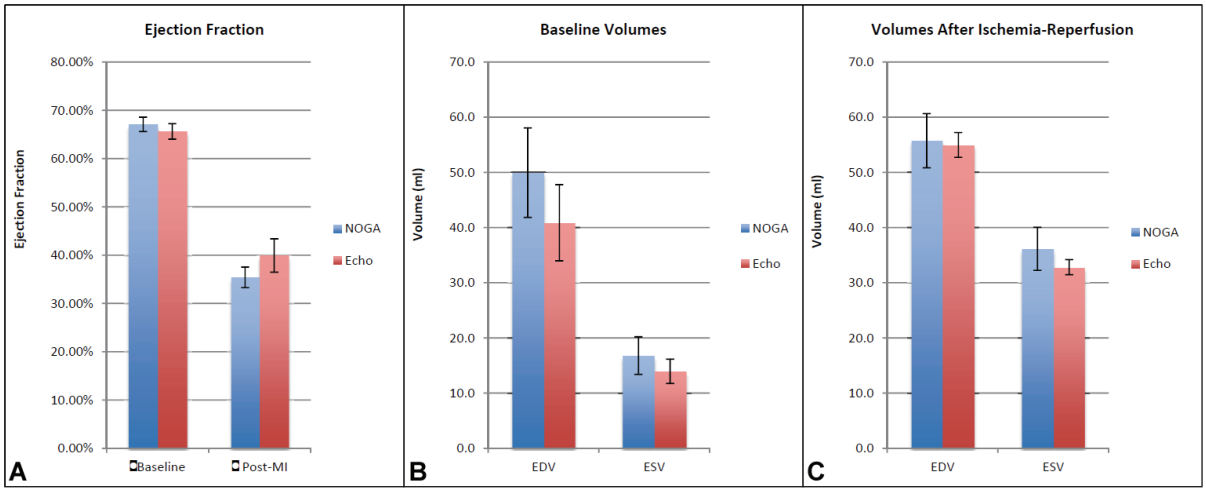

Figure 5. Comparison of Echo measurements to NOGA: A) Ejection fraction measured at baseline and after ischemia-reperfusion shows no significant difference between echo and NOGA. B) Baseline volumes and C) volumes after ischemia-reperfusion shows no difference between echo and NOGA.

significant decline in EF after ischemia-reperfusion, along with dilatation and increased heart volumes after ischemia-reperfusion corroborated by echo and gross morphometric findings.

The Myostar catheter accurately delivers therapeutics via transendocardial injection [13-19]. Our findings confirm that, with localization and identification of the ischemic border zone by NOGA mapping, the Myostar catheter can be an effective method for delivering therapeutics after acute myocardial injury. When examined on gross morphometric analysis, transendocardial beads were detected in the ischemic border zone of the heart.

Limitations

The authors recognize some limitations of this study including the small sample size of 5 experimental subjects and 2 shams. Moreover, 4 animals were excluded due to technical issues along with 1 death. Although the numbers are limited, the findings demonstrated in this study are consistent and valid.

Conclusions

The NOGA mapping system and Myostar injection catheter provide a novel alternate treatment strategy in the burgeoning realm of ischemic heart disease [21]. Herein, we demonstrate that the NOGA catheter accurately measures cardiac function as compared to echo and can be a modality in assessing the severity of ischemic injury. Furthermore, in combination with the Myostar catheter, it can be used to accurately deliver therapeutics to targeted sites of endocardium.

Address correspondence to: Dr. Jon C. George, Adjunct Research Instructor, Cardiovascular Research Center, Temple University School of Medicine, 3500 N. Broad Street, MERB 1040, Philadelphia, PA 19140, 215-707-4045; Director of Clinical Research, Interventional Cardiology and Endovascular Medicine, Deborah Heart and Lung Center, 200 Trenton Road, Browns Mills, NJ 08015, 609-735-2907 E-mail: jcgeorgemd@hotmail.com

References

[1] Murray CJ, Lopez AD. Mortality by cause for eight regions of the world: Global Burden of Disease Study. Lancet 1997; 349: 1269-1276.

[2] Glogar H, Gyongyos IM. Austrian Journal of Cardiology 2010 Glogar HDNon-fluoroscopic catheter-based endocardial mapping and mapping-guided percutaneous transmyocardial revascularization. 12, 2001: pp: 503-508.

[3] Callans DJ, Ren JF, Michele J, Marchlinski FE, Dillon SM. Electroanatomic Left Ventricular Mapping in the Porcine Model of Healed Anterior Myocardial Infarction : Correlation With Intracardiac Echocardiography and Pathological Analysis. Circulation 1999; 100: 1744-1750.

[4] Gepstein L, Goldin A, Lessick J, Hayam G, Shpun S, Schwartz Y, Hakim G, Shofty R, Turgeman A, Kirshenbaum D, Ben-Haim SA. Electromechanical Characterization of Chronic Myocardial Infarction in the Canine Coronary Occlusion Model. Circulation 1998; 98: 2055-2064.

[5] Gepstein L, Hayam G, Ben-Haim SA. A Novel Method for Nonfluoroscopic Catheter-Based Electroanatomical Mapping of the Heart: In Vitro and In Vivo Accuracy Results. Circulation 1997; 95: 1611-1622.

[6] Gyongyosii M, Sochor H, Khorsand A, Gepstein L, Glogar D. Online Myocardial Viability Assessment in the Catheterization Laboratory via NOGA Electroanatomic Mapping. Circulation 2001; 104: 1005-1011.

[7] Koch KC, vom Dahl J, Wenderdel M, Nowak B, Schaefer WM, Sasse A, Stellbrink C, Buell U, Hanrath P. Myocardial viability assessment by endocardial electroanatomic mapping: comparison with metabolic imaging and functional recovery after coronary revascularization. J Am Coll Cardiol 2001; 38: 91-98.

[8] Kornowski R, Hong MK, Leon MB. Comparison Between Left Ventricular Electromechanical Mapping and Radionuclide Perfusion Imaging for Detection of Myocardial Viability. Circulation 1998; 98: 1837-1841.

[9] Kornowski R, Baim DS, Moses JW, Hong MK, Laham RJ, Fuchs S, Hendel RC, Wallace D, Cohen DJ, Bonow RO, Kuntz RE, Leon MB. Short- and Intermediate-Term Clinical Outcomes From Direct Myocardial Laser Revascularization Guided by Biosense Left Ventricular Electromechanical Mapping. Circulation 2000; 102: 1120-1125.

[10] Kornowski R, Hong MK, Gepstein L, Goldstein S, Ellahham S, Ben-Haim SA, Leon MB. Preliminary Animal and Clinical Experiences Using an Electromechanical Endocardial Mapping Procedure to Distinguish Infarcted From Healthy Myocardium. Circulation 1998; 98: 1116-1124.

[11] Vale PR, Losordo DW, Milliken CE, Maysky M, Esakof DD, Symes JF, Isner JM. Left Ventricular Electromechanical Mapping to Assess Efficacy of phVEGF165 Gene Transfer for Therapeutic Angiogenesis in Chronic Myocardial Ischemia. Circulation 2000; 102: 965-974.

[12] Vale PR, Losordo DW, Milliken CE, McDonald MC, Gravelin LM, Curry CM, Esakof DD, Maysky M, Symes JF, Isner JM. Randomized, Single-Blind, Placebo-Controlled Pilot Study of Cathe-

ter-Based Myocardial Gene Transfer for Therapeutic Angiogenesis Using Left Ventricular Electromechanical Mapping in Patients With Chronic Myocardial Ischemia. Circulation 2001; 103: 2138-2143.

[13] Beeres SL, Beeres SL, Bax JJ, Dibbets P, Stokkel MP, Zeppenfeld K, Fibbe WE, van der Wall EE, Schalij MJ, Atsma DE. Effect of intramyocardial injection of autologous bone marrow-derived mononuclear cells on perfusion, function, and viability in patients with drug-refractory chronic ischemia. Journal of Nuclear Medicine 2006; 47: 574-580.

[14] Dib N, Dinsmore J, Lababidi Z, White B, Moravec S, Campbell A, Rosenbaum A, Seyedmadani K, Jaber WA, Rizenhour CS, Diethrich E. One-Year Follow-Up of Feasibility and Safety of the First U.S., Randomized, Controlled Study Using 3-Dimensional Guided Catheter-Based Delivery of Autologous Skeletal Myoblasts for Ischemic Cardiomyopathy (CAuSMIC Study). J Am Coll Cardiol Intv 2009; 2: 9-16.

[15] Krause KT, Jaquet K, Geidel S, Schneider C, Mandel C, Stoll HP, Hertting K, Harle T, Kuck KH. Percutaneous endocardial injection of erythropoietin: Assessment of cardioprotection by electromechanical mapping. European Journal of Heart Failure 2006; 8: 443-450.

[16] Perin EC, Silva GV, Fernandes MR, Munger T, Pandey A, Sehra R, Talcott M, Bichard CJ, Creed J, Wong JW, Oliveira EM, Zheng Y, Canales J, Cardoso CO, Patterson MS, Serruys PW. First experience with remote left ventricular mapping and transendocardial cell injection with a novel integrated magnetic navigation-guided electromechanical mapping system. EuroIntervention 2007; 3: 142-148.

[17] Perin EC, Dohmann HF, Borojevic R, Silva SA, Sousa AL, Mesquita CT, Rossi MI, Carvalho AC, Dutra HS, Dohmann HJ, Silva GV, Belém L, Vivacqua R, Rangel FO, Esporcatte R, Geng YJ, Vaughn WK, Assad JA, Mesquita ET, Willerson JT. Transendocardial, Autologous Bone Marrow Cell Transplantation for Severe, Chronic Ischemic Heart Failure. Circulation 2003; 107: 2294-2302.

[18] Smits PC, van Geuns RJ, Poldermans D, Bountioukos M, Onderwater EE, Lee CH, Maat AP, Serruys PW. Catheter-Based intramyocardial injection of autologous skeletal myoblasts as a primary treatment of ischemic heart failure: Clinical experience with Six-Month Follow-Up. J Am Coll Cardiol 2003; 42: 2063-2069.

[19] Gepstein L, Hayam G, Shpun S, Ben-Haim SA. Hemodynamic Evaluation of the Heart With a Nonfluoroscopic Electromechanical Mapping Technique. Circulation 1997; 96: 3672-3680.

[20] Schiller NB, Shah, PM, Crawford M, DeMaria A, Devereux R, Feigenbaum H, Gutgesell H, Reichek N, Sahn D, Schnittger I. Recommendations for quantitation of the left ventricle by two -dimensional echocardiography. American Society of Echocardiography Committee on Standards, Subcommittee on Quantitation of Two-Dimensional Echocardiograms. J Am Soc Echocardiogr 1989; 5: 358-367.

[21] Lloyd-Jones D, Adams R, Carnethon M, De Simone G, Ferguson TB, Flegal K, Ford E, Furie K, Go A, Greenlund K, Haase N, Hailpern S, Ho M, Howard V, Kissela B, Kittner S, Lackland D, Lisabeth L, Marelli A, McDermott M, Meigs J, Mozaffarian D, Nichol G, O'Donnell C, Roger V, Rosamond W, Sacco R, Sorlie P, Stafford R, Steinberger J, Thom T, Wasserthiel-Smoller S, Wong N, Wylie-Rosett J, Hong Y; American Heart Association Statistics Committee and Stroke Statistics Subcommittee. Heart Disease and Stroke Statistics, 2009 Update. Circulation 2009; 119: 480-486.